XVIIIèmes Journées Nationales Génie Côtier – Génie Civil
Anglet, 2024
DOI:10.5150/jngcgc.2024.050 © *Editions Paralia CFL*
disponible en ligne – http://www.paralia.fr – available online

Ultra-high-resolution bathymetry estimation using a visible airborne drone, photogrammetry and neural network

Antoine COLLIN [1], Dorothée JAMES [1], Nancy LAMONTAGNE [1], Renaud HARDY [1], Coralie MONPERT [2], Eric FEUNTEUN [1]

1. Centre de GéoEcologie Littorale, EPHE-PSL Université, 15 boulevard de la mer, 35800 Dinard, France.
   (antoine.collin ; dorothee.james ; nancy.lamontagne ; eric.feunteun)@ephe.psl.eu
2. Shom, Service Hydrographique et Océanographique de la Marine, 13 Rue du Châtellier, 29200 Brest, France.
   coralie.monpert@shom.fr

Abstract:
The knowledge of the bathymetry draws great attention of worldwide stakeholders tasked with trade and leisure navigation, oceanography, ecology, or coastal planning facing climate change. Solely 15% of the rivers, seas or oceans have been mapped using accurate and precise methodology, based on conventional waterborne sonar and airborne lidar. Satellite-derived bathymetry has therefore prospered for the last two decades but still provides spatially-coarse by-products.
We propose to develop the UAV-derived bathymetry (UDB) to get centimeter-scale (ultra-high resolution) digital depth maps to match subtle but valuable geo-ecological processes. The coral reef lagoon of Grandes Cayes (Saint-Martin Island in French Lesser Antilles) represented the study site.
Using a consumer-grade multispectral UAV, several inversion techniques were tested and compared: photogrammetrical structure-from-motion, semi-analytical ratio transform, and empirical regression. Ground-truth airborne bathymetric lidar were randomly split into calibration, validation and test sub-datasets.
The ratio transform (R^2=0,01), photogrammetry (R^2=0,41), linear regression (R^2=0,67), and combination of both latter ones (R^2=0,74) increasingly predicted bathymetry from 0 to -2,5 m depth. The UDB was further refined by merging the photogrammetry with a nonlinear regression (one-layer three-neuron network), attaining a R^2=0,84, and a vertical accuracy of 0,2 m.

Keywords:
Bathymetry, Unmanned aerial vehicle, Coral reefs, Saint-Martin, Ratio transform, Photogrammetry, Structure-from-motion, Perceptron, Neural network.

1. Introduction

1.1 Bathymetry mapping

Living on our blue Planet (covered by 71% of water), the knowledge of the seabed remains drastically poorer compared to this of the land realm. Only 15% of the rivers, seas or oceans have been surveyed by reliable sonar or lidar technology (WÖLFL *et al.*, 2019). This paucity strongly impedes the understanding and informed management of the riverine and coastal risks, as well as the biodiversity preservation in the context of sea-level rise (FIRTH *et al.*, 2016).
Conventional mapping relies on acoustic waterborne campaign (LE QUILLEUC *et al.*, 2023), active optical airborne survey (COLLIN *et al.*, 2023d), passive optical airborne (COLLIN *et al.*, 2023a) and spaceborne acquisition (COLLIN & PLANES, 2011). The cost per surface area obviously highlights the satellite imagery to be selected for shallow coastal areas bathed by clear-to-moderately clear waters. Even if the spaceborne imagery has gained in radiometric (COLLIN *et al.*, 2016), temporal (COLLIN *et al.*, 2023c), spectral (COLLIN *et al.*, 2017; COLLIN *et al.*, 2023b), and spatial (COLLIN & HENCH, 2012; COLLIN *et al.*, 2014) resolutions over the last two decades, bathymetric by-products can maximally reach pixel size of 1,2 m in native or 0,3 m in pansharpened mode, deemed as less reliable.

1.2 Ultra high-resolution bathymetry mapping

The spatially-explicit bathymetry at finer spatial resolution is compulsorily attained with an unmanned airborne vehicle (UAV), capable of collecting centimetre-scale data over very shallow-to-shallow waters, unsurvey able by any waterborne, even light, craft. Various approaches can be considered to retrieve the bathymetry from UAV:

a) Photogrammetrical: by applying the structure-from-motion technique, a 0,008-km^2 coral reef lagoon in French Polynesia was mapped with 0,45-m accuracy down to 1,8-m depth (CASELLA *et al.*, 2017).
b) Empirical: from machine learning, a support vector regression helped to improve the refraction-driven bathymetry underestimation affecting the photogrammetric product over two sites in Greece with 0,4 m accuracy until 5-m depth, and 2,2-m accuracy until 15-m depth (AGRAFIOTIS *et al.*, 2019).
c) Semi-analytical: based on an optimized band ratio analysis, stemmed from the ratio transform (STUMPF *et al.*, 2003), a 0,5-km^2 coastal area in Italy was mapped with 0,2-m vertical accuracy down to 5-m depth (ROSSI *et al.*, 2020).
d) Analytical: using a physics-based framework (underwater spectroradiometer and water colour simulation, WASI, software, GEGE, 2014), three study areas in Greece were mapped with 0,4-m vertical accuracy also down to 5-m depth (ALEVIZOS *et al.*, 2022).

1.3 Comparative analysis and synergy in ultra-high-resolution bathymetry mapping
Since the various approaches, applied to UAV-derived bathymetry (UDB), were carried out over different sites with distinct materials, this research will innovatively compare the conventional UDB methods (semi-analytical, photogrammetrical, and empirical) over the same site and will propose an original strategy to synergistically combine the best methods.

2. Methodology

2.1 Study site
The experiments took place over the 0,02-km^2 fringing reef of the Grandes Cayes along the shore of Saint-Martin Island (18°6'55'' N; 63°1'14'' W) (Figure 1).

2.2 UAV data and processing
The UAV flight was undertaken with a consumer-grade (5 k €/$) DJI Phantom 4 MultiSpectral-RTK leveraging one blue-green-red (BGR) channel, one blue (B, 450 nm ± 16 nm); one green (G, 560 nm ± 16 nm); one red (R, 650 nm ± 16 nm); one red edge (RE, 730 nm ± 16 nm); and one near-infrared (NIR, 840 nm ± 26 nm). Each channel acquires 2,1 mega pixels. An array of 799 imageries (each composed of the 6 images) was built using the flight planning software DJI Ground Station Pro: 80% and 70% front and side overlapping, respectively. At a height of 50 m, this corresponds to a pixel size of 0,03 m.
The orthorectification (WGS84, UTM 20N) of each imagery was ensured by the RTK centimetre-scale geopositioning inherited from the D-RTK2 station and the D-RTK UAV antennas. The radiometric correction, enabling to produce reflectance imagery, resulted from the ratio between the radiance acquired by the six nadiral channels and the irradiance simultaneously measured by the zenithal pyranometer. In addition, a calibration panel was captured before and after the flight.
The photogrammetry procedure was applied to the dataset so as to obtain the digital surface model (DSM) and the multispectral orthomosaics. The DJI Terra software was parameterized to, first, integrate the scene and calibration imageries in the aero-triangulation and cloud densification processes, then map the DSM and orthomosaics in the WGS84 datum, locally projected in UTM 20N.

2.3 Lidar data and processing
The UDB by-products were calibrated, validated and tested using a topobathymetric lidar dataset collected and processed by the Shom in 2018 and 2019, respectively (SHOM-IGN, 2019, doi.org/10.17183/L3D_SAINT_MARTIN_2019). Provided with at least 4 points.m^{-2}, the bathymetric point cloud was rasterized at 0,03-m pixel size into the WGS84 datum projected in UTM20N (Figure 1).

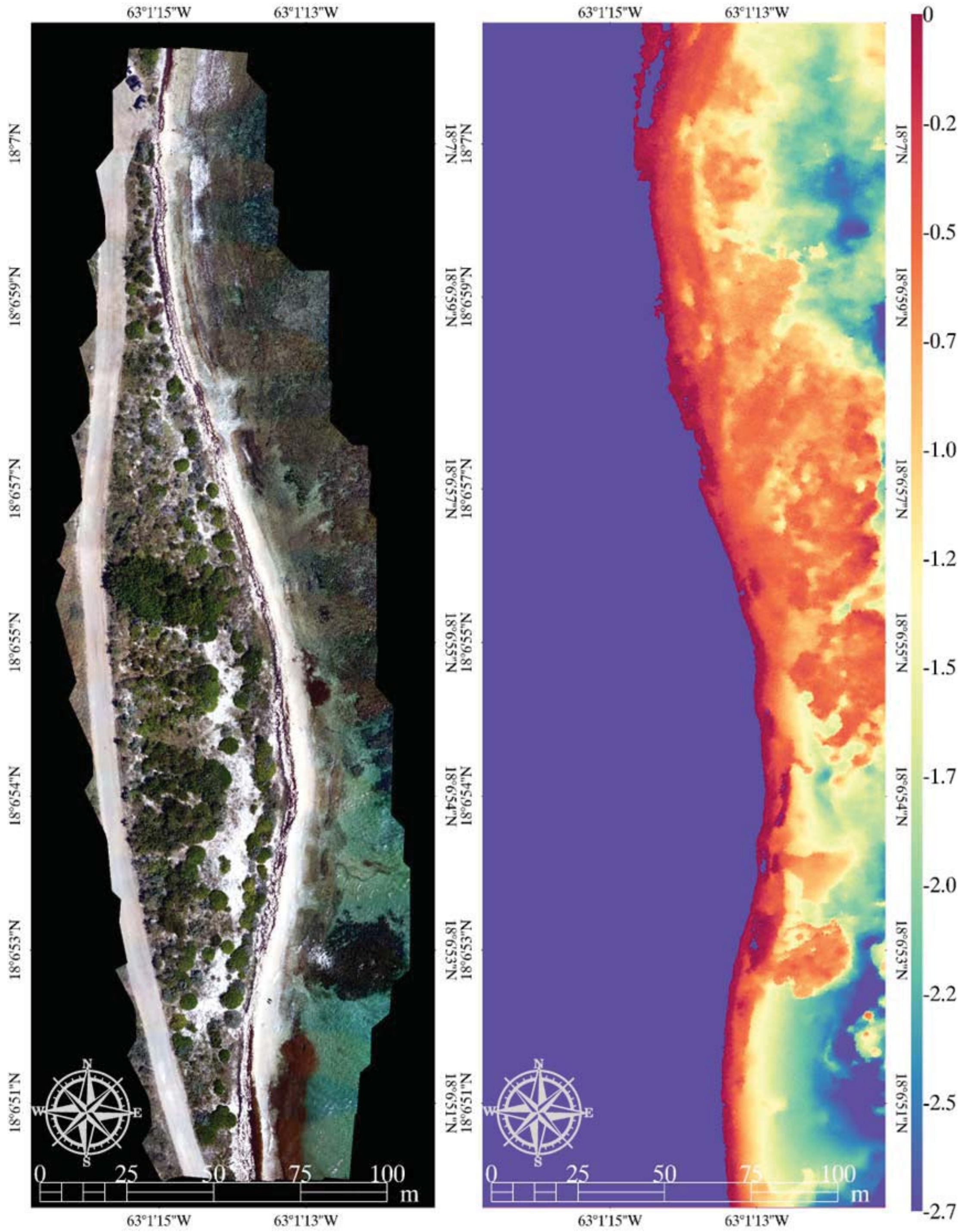

Figure 1. Left: Natural-coloured orthomosaic of the fringing reef of Grandes Cayes (Saint-Martin Island) derived from 799 imageries collected by the Phantom 4 MultiSpectral-RTK. Right: Bathymetric lidar imagery of the fringing reef of Grandes Cayes (Saint-Martin Island) rasterized from topobathymetric lidar point clouds collected by the Phantom 4 MultiSpectral-RTK (4216×12373 pixels, 0,03 m pixel size).

2.4 Algorithms for the bathymetry retrieval

In addition to the photogrammetrical approach, the ratio transform and the regression techniques were tested. The ratio transform constitutes a semi-analytical procedure based on the differential water absorption by waveband (STUMPF *et al.*, 2003). Basically, from blue to near-infrared, the shorter the wavelength is, the deeper the light propagates. This principle is true for clear waters but has to be mitigated for waters laden with inorganic/organic dissolved/particulate components. The regression portrays the empirical procedure, in which numerical values of a response (or dependent variable) are modelled by one (or many) predictor(s). The model, searching to minimize the numerical differences between training values of response and predictor(s), can be linear (used to compare the four UDB methods) or nonlinear (used to deepen the best UDB method with a one-layer three-neuron perceptron, representing the neural network, COLLIN & HENCH, 2012).

2.5 Comparison methodology

The bathymetric lidar dataset was randomly divided into three even sub-datasets: 28 496 calibration pixels, 28 496 validation pixels, and 28 497 test pixels. Each of the four UDB methods were compared using the independent test sub-dataset, following their training with both previous sub-datasets.

3. Results

3.1 Performances of the four approaches

The three conventional approaches yielded very contrasted performances: very low accuracy for ratio transform (R^2=0,01), poor accuracy for photogrammetry (R^2=0,41), medium accuracy for linear regression (R^2=0,67). Merging the photogrammetry-derived DSM with BGR information in a linear regression provided high accuracy (R^2=0,74) (Figure 2).

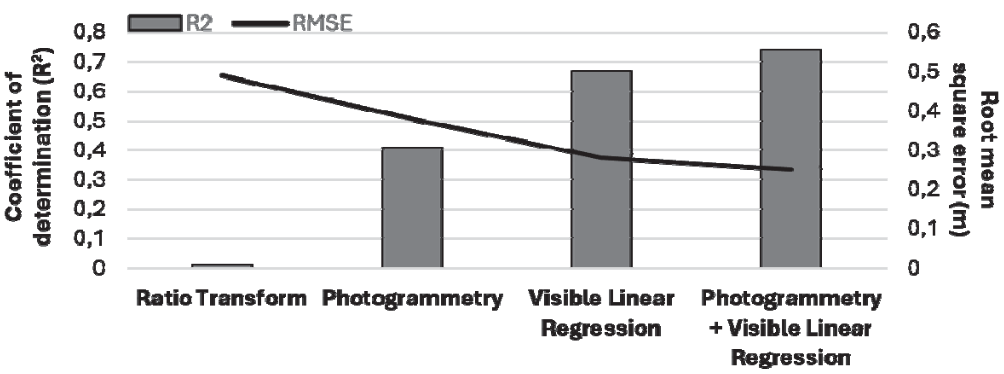

Figure 2. Bar plot of the performance of the three conventional UAV-derived bathymetry and proposed fusion of photogrammetrical and empirical approaches.

3.2 Increasing the performance of the combined approach

The prediction of the combined approach was further refined by adopting a nonlinear model, based on a one-layer three-neuron network (R^2=0,84), which is trivial but more transferable (Figure 3). The RMSE of 0,2 m encompassed the 2,5-m depth range.

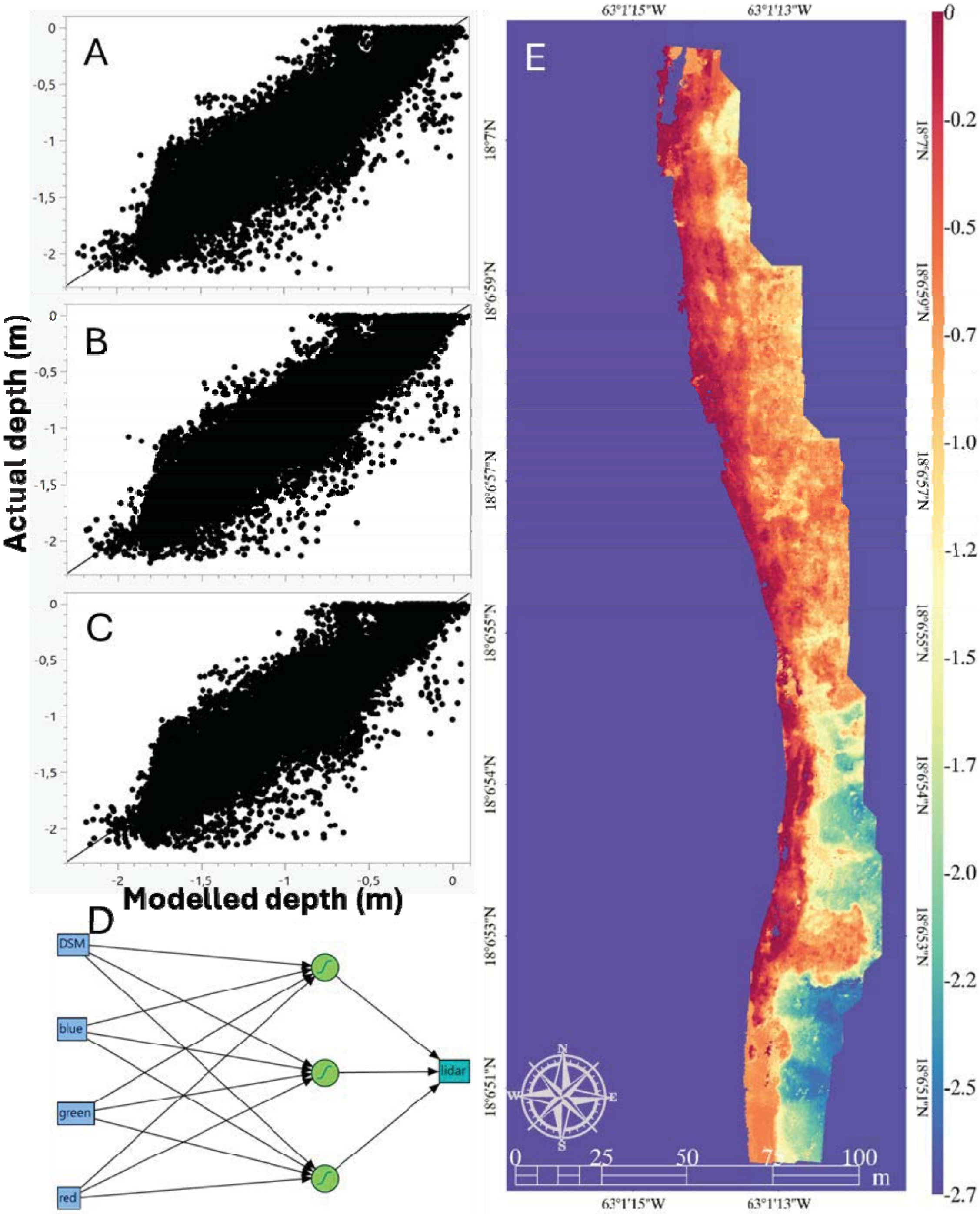

Figure 3. Actual and modelled depths for the (A) training, (B) validation, and (C) test sub-datasets, based on (D) the one-layer three-neuron network. (E) Spatial model.

4. Conclusions

The shallow bathymetry of a coral reef lagoon (Grandes Cayes, Saint-Martin Island) was successfully predicted (R^2=0,84) by the combination of an RTK UAV-derived photogrammetry and nonlinear regression (one-layer three-neuron perceptron) methodology. That fusion enabled to map the 0-to-2,5-m depth range with a 0,2 m vertical accuracy at 0,03-m spatial resolution. When isolated, the photogrammetry and linear regression yielded R^2 of 0,41 and 0,67, but reached R^2 of 0,74, when merged. Those results were constrained by clear waters above shallow seabeds populated by hard substrata. We propose to deepen findings by using narrower bands, provided by a superspectral or hyperspectral sensor, to add the mapped inherent optical properties of seawater into the combination of the photogrammetric DSM and reflectance predictors.

5. References

AGRAFIOTIS P, SKARLATOS D., GEORGOPOULOS A., KARANTZALOS K. (2019). *Shallow Water Bathymetry Mapping from Uav Imagery Based on Machine Learning*. ISPRS Int. Arch. Photogramm. Remote Sens. Spat. Inf. Sci., Vol. XLII-2/W10, pp 9-16. doi.org/10.3390/rs12020322

ALEVIZOS E, OIKONOMOU D, ARGYRIOU A.V., ALEXAKIS D.D. (2022*). Fusion of Drone-Based RGB and Multi-Spectral Imagery for Shallow Water Bathymetry Inversion*. Remote Sensing, Vol. 14, p 1127. doi.org/10.3390/rs14051127

CASELLA E., COLLIN A., HARRIS D., FERSE S., BEJARANO S., PARRAVICINI V., HENCH J.L., ROVERE A. (2017). *Mapping coral reefs using consumer-grade drones and structure from motion photogrammetry techniques*. Coral Reefs, Vol. 36, pp 269–275. doi.org/10.1007/s00338-016-1522-0

COLLIN A., BULOT A., PASTOL Y., LE GOFF L., FEUNTEUN E. (2023a). *Classification des habitats benthiques par segmentation sémantique d'imagerie optique et LiDAR ouverte : Ortho-Littorale et Litto3D en baie de Saint-Malo*. 4th merIGéo, Le Havre, pp 44-47.

COLLIN A., ETIENNE S., FEUNTEUN E. (2017). *VHR coastal bathymetry using WorldView-3: colour versus learner*. Remote Sensing Letters, Vol. 8(11), pp 1072-1081. doi.org/10.1080/2150704X.2017.1354261

COLLIN A., HENCH J. (2012). *Towards deeper measurements of tropical reefscape structure using the WorldView-2 spaceborne sensor*. Remote Sensing, Vol. 4(5), pp 1425-1447. doi.org/10.3390/rs4051425

COLLIN A., JAMES D., FEUNTEUN E. (2023b). *Pléiades Neo-derived bathymetry in coastal temperate waters: the case study of Saint-Malo*. Proceedings of the 5th International Electronic Conference on Remote Sensing, On-line, 7–21 November. doi:10.3390/ECRS2023-16366

COLLIN A., LAPORTE J., KOETZ B., MARTIN-LAUSZER F.R., DESNOS Y.L. (2016). *Mapping bathymetry, habitat and potential bleaching using Sentinel-2*. 13th International Coral Reef Symposium, Honolulu, pp 416-430.

COLLIN A., NADAOKA K., NAKAMURA T. (2014). *Mapping VHR Water Depth, Seabed and Land Cover Using Google Earth Data*. ISPRS Int. J. Geo-Inf., Vol. 3(4), pp 1157-1179. doi.org/10.3390/ijgi3041157

COLLIN A., PALOLA P., JAMES D., PASTOL Y., MONPERT C., LOYER S., STOLL B., FEUNTEUN E., WEDDING L. (2023c). *Superdove-modelled bathymetry using neural networks along a turbidity gradient: Bréhat, Saint-Barthélémy and Tetiaroa islands*. The International Archives of the Photogrammetry, Remote Sensing and Spatial Information Sciences, Vol. 48, pp 1351-1356. doi.org/10.5194/isprs-archives-XLVIII-1-W2-2023-1351-2023

COLLIN A., PASTOL Y., LETARD M., LE GOFF L., GUILLAUDEAU J., JAMES D., FEUNTEUN E. (2023d). *Increasing the Nature-Based Coastal Protection Using Bathymetric Lidar, Terrain Classification, Network Modelling: Reefs of Saint-Malo's Lagoon?*. In: Niculescu, S. (eds) European Spatial Data for Coastal and Marine Remote Sensing. Springer, Cham. doi.org/10.1007/978-3-031-16213-8_17

COLLIN A., PLANES S. (2011). *What is the value added of 4 bands within the submetric remote sensing of tropical coastscape? QuickBird-2 vs WorldView-2?* IEEE International Geoscience and Remote Sensing Symposium, Vancouver, pp 2165-2168. doi.org/10.1109/IGARSS.2011.6049595

FIRTH L.B., KNIGHTS A.M., BRIDGER D., EVANS A., MIESKOWSKA N., et al. (2016). *Ocean sprawl: challenges and opportunities for biodiversity management in a changing world*. Oceanography and Marine Biology: an annual review, Vol. 54, pp 189-262. doi.org/10.1201/9781315368597-9

GEGE P. (2014). *WASI-2D: A software tool for regionally optimized analysis of imaging spectrometer data from deep and shallow waters*. Computers & Geosciences, Vol. 62, pp 208-215. doi.org/10.1016/j.cageo.2013.07.022

LE QUILLEUC A., HUSSET M.-C., COLLIN A., FEUNTEUN E. (2023). *Cartographie prédictive d'un coquillage invasif via l'apprentissage automatique des données acoustiques multi-fréquentielles et vérités-terrain : Crepidula fornicata en Baie du Mont-Saint-Michel*. 4th merIGéo, le Havre, pp 165-167.

ROSSI L., MAMMI I., PELLICIA F. (2020). *UAV-Derived Multispectral Bathymetry*. Remote Sensing, Vol. 12, p 3897. doi.org/10.3390/rs12233897

STUMPF R.P., HOLDERIED K., SINCLAIR M. (2003). *Determination of water depth with high-resolution satellite imagery over variable bottom types*. Limnol. Oceanogr. Vol. 48, pp 547–556. doi.org/10.4319/lo.2003.48.1_part_2.0547

WOLFL A.-C., SNAITH H., AMIREBRAHIMI S., DEVEY C.W., …, WIGLEY R. (2019). *Seafloor mapping the challenge of a truly global ocean bathymetry*. Frontiers in Marine Science, Vol. 6, p 283. doi.org/10.3389/fmars.2019.00283